minerals

MDPI

Article

The Mid-Cretaceous Tectonothermal Evolution of the Zhangbaling Tectonic Belt, East China: Evidence from Zircon (U–Th)/He and Detrital Zircon U–Pb Dating

Yongsheng Wang *, Qiao Bai, Weiwei Ma, Juanhao Yang and Zhensheng Li

School of Resources and Environmental Engineering, Hefei University of Technology, Hefei 230009, China; joebai@126.com (Q.B.); ma_wei7@163.com (W.M.); jiaqiangyang1995@163.com (J.Y.); lizhensh@163.com (Z.L.)
* Correspondence: yshw9007@hfut.edu.cn

Abstract: The Zhangbaling tectonic belt (ZTB), one of the most representative tectonic belts in East China, has experienced uplift since the Early Cretaceous and is, thus, an excellent object for understanding the tectonic uplift and topographical evolution of East China and the whole of East Asia. On the basis of field observations, in this contribution to the literature, we carried out detrital zircon LA-ICP-MS U–Pb dating for the Upper Cretaceous sediments in the basins adjacent to the ZTB and zircon (U–Th)/He dating for the Early Cretaceous plutons along the western flank of this belt. Detailed field observation showed that the orthogneiss of the Feidong Complex experienced sinistral strike–slip activities, while the marbles underwent thrusting; thrust faults were developed in the Early Cretaceous plutons and volcanic rocks, and normal faults were superimposed on thrust or strike–slip faults. The detrital zircon dating results showed that the Upper Cretaceous sediments are characterized by an Early Cretaceous major cluster with just a minor cluster from the middle Neoproterozoic ages, indicating that the Zhangbaling Group and the Feidong Complex of the ZTB are not their main provenance. Zircon (U–Th)/He dating results showed that the ZTB experienced rapid uplifting during the mid-Cretaceous and recorded another rapid uplifting after 30 Ma. Combining existing research with our new data, it can be concluded that the ZTB was characterized by thrust activity in the mid-Cretaceous, which occurred under regional compression setting and was the basis of the formation of a watershed after 30 Ma.

Keywords: Zhangbaling tectonic belt; zircon (U–Th)/He geochronology; detrital zircon U–Pb dating; mid-Cretaceous compression

Citation: Wang, Y.; Bai, Q.; Ma, W.; Yang, J.; Li, Z. The Mid-Cretaceous Tectonothermal Evolution of the Zhangbaling Tectonic Belt, East China: Evidence from Zircon (U–Th)/He and Detrital Zircon U–Pb Dating. *Minerals* **2023**, *13*, 1142. https://doi.org/10.3390/min13091142

Academic Editor: Simon Paul Johnson

Received: 5 August 2023
Revised: 19 August 2023
Accepted: 25 August 2023
Published: 30 August 2023

1. Introduction

The East Asian continent was sandwiched between several plates during the late Mesozoic era, and its Cenozoic tectonic evolution was mainly controlled by the continent–continent collision in the Neotethys tectonic domain to the west and the subduction of the Paleo-Pacific Plate to the east [1–3]. Three topographic ladders developed from west to east in China, indicating that the far-field stress generated by the Neotethys tectonic domain was essential for the development of the current topography. A significant number of low-temperature thermochronology results have shown that many mountains in East China, away from the Neotethys tectonic domain and with different formation times, such as the Wutai Mountain [4], Yanshan Mountain [5], Taishan Mountain [6], Dabie Mountains [7], Huangshan Mountain [8], and Yunkai Mountains [9], have all experienced rapid uplifting since the Paleocene. This corresponded to the beginning of the continent–continent collision between the Indian and Eurasian plates [10,11], indicating that the Neotethys tectonic domain has controlled the formation of the current topography since the Paleocene. However, the late Mesozoic evolution of the East Asian continent was mainly controlled by the subduction of the Paleo-Pacific Plate [12–15]. Regional angular unconformity between the Upper and Lower Cretaceous occurred widely in East Asia [12,16–18], which was

generally related to the mid-Cretaceous (~100 Ma) global plate reorganization event [19–21]. Although it is still controversial whether there was a plateau in East China during the late Mesozoic era [22,23], the topographical pattern was obviously different from the current one. Therefore, what role did the subduction of the Paleo-Pacific Plate play in the development of the current topography of East Asia? Did the formation of the current topography begin in the mid-Cretaceous? Was the tectonic setting of the mid-Cretaceous compression or extension? Answers to these questions are helpful to better understand the tectonic evolution and dynamic background of the East Asian continent since the late Mesozoic era.

The NNE–SSW-striking Zhangbaling tectonic belt (ZTB) is located along the boundary between the North China Block (NCB) and the South China Block (SCB), and sandwiched between the Dabie Orogen and the Sulu Orogen (Figure 1); thus, it is one of most important tectonic belts in East China [24]. Recent detrital zircon dating results showed that the Lower Cretaceous Zhuxiang Formation to the west of the ZTB is mainly of the Early Cretaceous age with just a few results from the Neoproterozoic age [25]. It is worth noting that the ZTB is characterized by a major Neoproterozoic cluster in its detrital zircon age frequency [26–29]. Clearly, Neoproterozoic rocks in the ZTB are not the main provenance of the strata to the west. Early Cretaceous magmatic rocks in the ZTB and surrounding areas, including plutons along the Tan–Lu Fault Zone and volcanic rocks in the Chuzhou area (Figure 1), may be other potential provenances. However, these plutons are closely linked with the Zhangbaling Group and the Feidong Complex in the ZTB and, thus, do not only provide Early Cretaceous minerals in sedimentary rocks. Therefore, the main provenance of the Cretaceous strata in the eastern Hefei Basin should be Early Cretaceous volcanic rocks. This further indicates that the ZTB may not show signs of a watershed in the earlier Late Cretaceous, and this causes the Chuzhou volcanic rocks to provide source materials for the sediments in the eastern Hefei Basin. On the basis of the above analysis, the ZTB is an excellent object of study that can provide important information on the topographical evolution of East China and East Asia since the Early Cretaceous.

In this contribution, on the basis of detailed field investigation, Upper Cretaceous sedimentary rocks in basins to the east and west of the ZTB were collected to carry out detailed detrital zircon LA-ICP-MS U–Pb dating, while Early Cretaceous plutons along the Tan–Lu Fault Zone were collected to carry out zircon (U–Th)/He dating. These new data provide new evidence regarding the tectonic uplift history of East Asia.

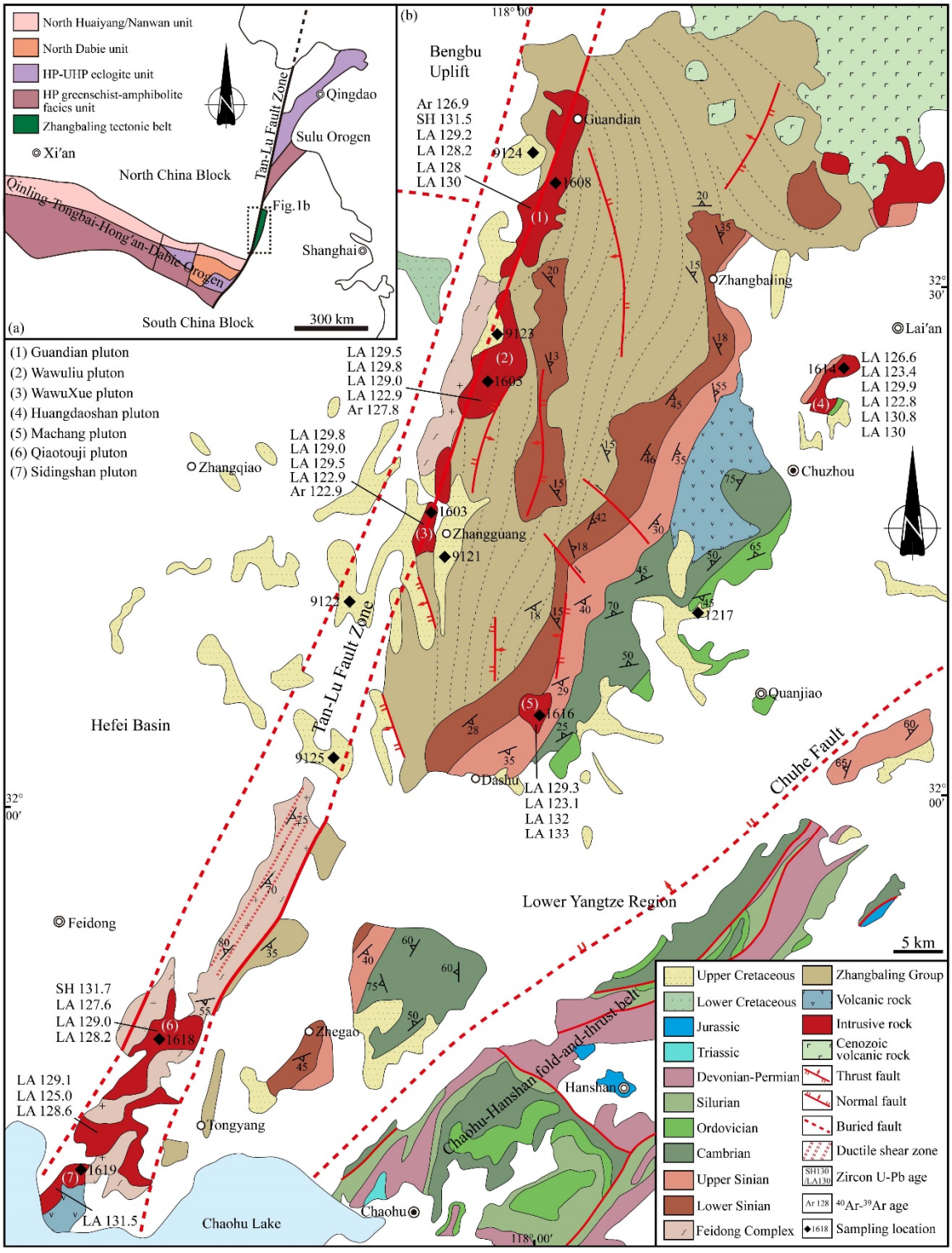

Figure 1. (**a**,**b**) Structural diagram of the ZTB and its surrounding areas. The black dashed line is the rock lineation trajectory of the Zhangbaling Group (after Zhang et al. [30]); the age of plutons is after Hu et al. [31], Jia et al. [32], Wang et al. [33], and Li et al. [34]).

2. Geological Setting

The NNE–SSW-striking ZTB, also known as the Zhangbaling Uplift [24], is located at the northwestern margin of the Lower Yangtze Region in the SCB (Figure 1). The ZTB is wide in the north and narrow in the south, generally showing a wedge shape

converging toward the SSW. It is separated from the Hefei Basin and the Bengbu Uplift on the southeastern margin of the NCB by the NE–SW-striking Tan–Lu Fault Zone to the west and adjacent to the Chaohu–Hanshan fold-and-thrust belt with the Chuhe Fault to the east [35]. Although there have been many different understandings about its formation mechanism [24,26,30,36,37], its formation time is generally believed to be the Triassic era, and its development was closely related to the continent–continent collision between the SCB and the NCB.

The ZTB is generally divided into two segments, namely, the northern Zhangbaling and the southern Zhangbaling, by the line of 32° N (Figure 1) [26,32]. The northern Zhangbaling is mainly composed of the Zhangbaling Group and the Sinian–Paleozoic sedimentary cover, while the southern Zhangbaling consists of the Feidong Complex and the Zhangbaling Group [27,29,35,37]. The Zhangbaling Group is mainly composed of metavolcanic rocks, phyllites, and metasandstones with protolith ages of ca. 750 Ma [26], which experienced Triassic greenschist–facies metamorphism and show gentle foliation in the outcrop [31,36,38]. The Feidong Complex is mainly made up of plagioclase amphibolite orthogneiss, biotite plagioclase gneiss, marble, and mica schist and experienced amphibolite–facies metamorphism [27]. The protolith of those orthogneiss included mainly Neoproterozoic rocks formed at 850~720 Ma [26,28,39] and a few Paleoproterozoic rocks [27,29].

The western margin of the northern Zhangbaling is cut by the NNE–SSW-striking brittle fault or ductile shear zone in the Tan–Lu Fault Zone, and a series of Early Cretaceous plutons developed along this zone [31–34]. The Sinian–Paleozoic sedimentary rocks cover the eastern part of the northern Zhangbaling and are in contact with the Zhangbaling Group through a large-scale detachment fault [26]. The Sinian rocks show relatively weak deformation with SE-dipping foliation. The Paleozoic strata are mainly composed of Cambrian and Ordovician rocks, which show intense folding, typically as comb-like chevron folds with NW-dipping axial plane and limbs [26,30,38]. Volumes of Mesozoic volcanic rocks crop out in the Chuzhou area (Figure 1), which cover the Sinian–Paleozoic sedimentary rocks and erupted between 132 and 116 Ma [40,41]. Mylonites occur widely in the orthogneiss of the Feidong Complex with steep foliation [42], while the marble generally exhibits brittle deformation. Muscovite $^{40}Ar/^{39}Ar$ ages from 245 Ma to 236 Ma in the orthogneiss indicate that the metamorphism and deformation mainly occurred during the Triassic era [30].

The Hefei Basin is located to west of the ZTB and north of the Dabie Orogen. The continent–continent collision of the NCB and the SCB resulted in the formation of a series of thrust faults and the early development of the Hefei Basin [43,44]. During the Early Cretaceous, these thrust faults were reactivated as normal faults, thus controlling deposition of the Cretaceous sediments in the Hefei Basin. During these two stages of fault activity, 5000–7000 m of terrestrial clastic deposits with volcanic rocks or pyroclastic rocks developed in the southern Hefei Basin [43–45]. The Tan–Lu Fault Zone, which cuts the western margin of the ZTB, was shown to be a normal fault, controlling the development of Cretaceous strata in the eastern Hefei Basin [46].

3. Field Characteristics and Sample Descriptions

Sedimentary rocks in the eastern Hefei Basin crop out mostly along the western flank of the ZTB, where they are mainly composed of the Upper Cretaceous Zhangqiao Formation and the Lower Cretaceous Zhuxiang Formation. Some rocks overlap above the Zhangbaling Group. The Zhuxiang Formation consists of purple–brown sandstone with silty mudstone. The Zhangqiao Formation includes two parts; the lower part is an alluvial fan deposit and consists of thick, massive, gray–purple, and poorly sorted conglomerate and pebbly sandstone [44], while the upper part is medium- to fine-grained sandstone with argillaceous siltstone and dips to the W or NW at 30° (Figure 2a). The clasts in the conglomerate are mainly composed of limestone, volcanic rock, gneiss, and phyllite, with sizes varying from 1 cm to 10 cm. The Upper Cretaceous Chishan Formation crops out to the east of the ZTB, which is also characterized by purple conglomerate with coarse-grain sandstone

in the lower part and sandstone and siltstone in the upper part. In this contribution, six sedimentary rock samples were collected, of which sample 1217 was taken from the Upper Cretaceous Chishan Formation to the east of the ZTB, and another five samples were taken from the Upper Cretaceous Zhangqiao Formation to the west (Figure 1).

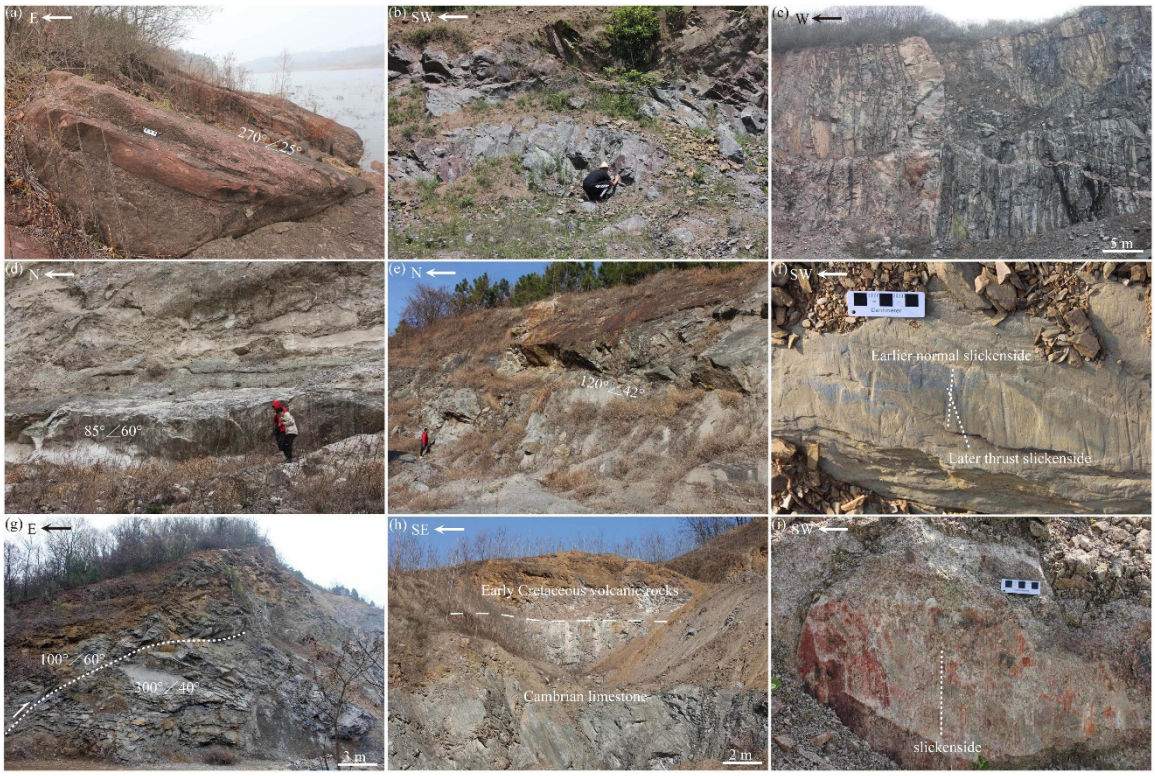

Figure 2. Field photos of the Zhangbaling tectonic belt. (**a**) Upper Cretaceous gravelly sandstone to the west of the ZTB; (**b**) many groups of faults developed in the diorite of Qiaotouji pluton; (**c**) steep ductile shear zones developed in the Feidong Complex; (**d**) fault activities in the marble exhibiting thrust faults prior to normal faults; (**e**) Sinian sediments with foliation dipping toward SE; (**f**) earlier normal slickensides and later thrust slickensides on the fault plane in the Sinian rocks; (**g**) SE-dipping thrust fault cutting the NW-dipping foliation; (**h**) Early Cretaceous volcanic rocks unconformably covering the Paleozoic strata; (**i**) thrust fault developed in Early Cretaceous pluton.

Several banded intrusion rocks are distributed in the northern Zhangbaling, which are exposed between the Cretaceous sedimentary rocks and the Zhangbaling Group, namely, from north to south, the Guandian, Wawuliu, and Wawuxue plutons (Figure 1). Volumes of plutons intrude into the Feidong Complex in the southern Zhangbaling, including the Qiaotouji pluton in the Feidong area and the Zhuyuanzhang, Sidingshan, Jimingshan, and Zhannongcun plutons on the north bank of Chaohu Lake [31–34]. Similar lithological characteristics are in these plutons, mainly monzogranite, granodiorite, quartz monzonite, and diorite, with emplacement times between 130 and 128 Ma (Figure 1). These plutons were cut by multiple groups of faults, resulting in the development of breccia and strong weathering. It should be noted that the occurrence of faults is variable, and there are significant differences in fault type at different outcrops. Moreover, each individual outcrop does not show a significant dominance of a certain fault (Figure 2b). Specifically, the Qiaotouji and Sidingshan plutons, intruding in the Feidong Complex, do not show the sinistral shear zone or brittle fault that were widely developed in the orthogneiss of the Feidong Complex. In addition, there are a few Early Cretaceous intrusion rocks in the central region and to the east of the ZTB, where the Machang pluton intruded into the Sinian rocks and the Huangdaoshan pluton exposed to the east of the ZTB (Figure 1). Seven

samples were collected, including the Guandian (1608), Wawuliu (1605), Wawuxue (1603), Qiaotouji (1618), Sidingshan (1619), Machang (1615), and Huangdaoshan (1614) plutons.

The Zhangbaling Group and the Feidong Complex exhibit different structural patterns. The Zhangbaling Group is charactered by gentle foliation with a dip angle of less than 20° and exhibits overall open folds. The orientation of the lineation varies gradually from NE-trending in the south to NW-trending in the north (Figure 1) [32]. Its dynamic mechanism can be explained as the partitioning of the triaxial deformation along an oblique convergent margin [33]. Steep ductile shear zones and brittle faults are widely developed in orthogneiss of the Feidong Complex in the southern Zhangbaling (Figure 2c). Thrust faults are generally developed in marble of the Feidong Complex (Figure 2d), and no steep strike–slip faults are superimposed or rebuilt.

The lower Sinian is mainly composed of low-grade metamorphic sandstone and phyllite, and the upper Sinian consists mainly of limestone and dolomite. The Sinian rocks dip generally SE or E at an angle between 20° and 50°, and there are detachment faults with a shear sense of the top to the SE. Detailed field observation shows that these faults occurred mostly along the foliation (Figure 2e), and two groups of slickensides show the later thrust fault superimposed on the earlier normal fault. The thrust slickensides obliquely cut the normal slickensides with angle of about 20° (Figure 2f). Paleozoic rocks are mainly composed of dolomite and limestone, which are generally shown as tight folds with W- or NW-dipping axial plane and limbs. A large number of thrust faults with NW-dipping occurred in Paleozoic rocks, and some were superimposed with later normal faults. It is worth noting that more SE-dipping thrust faults with shear sense of the top to the NW were also developed, and these faults cutting the NW-dipping foliation can be often observed in the outcrop (Figure 2g). In the Chuzhou area, large volumes of Early Cretaceous volcanic rocks are distributed to the east of the ZTB. Sinian and Paleozoic rocks are covered by volcanic rocks, and their boundary is nearly horizontal (Figure 2h). Thrust faults, with shear sense above the NW, have developed in both Early Cretaceous volcanic and intrusion rocks (Figure 2i).

4. Methodology and Analytical Results

Zircon crystals were separated at the Langfang Chengxin Geological Service Co., Ltd., Hebei, China. After crushing and heavy liquid separation, zircon separates were manually selected by binoculars for detrital zircon U–Pb dating and zircon (U–Th)/He (ZHe) dating.

4.1. Detrital Zircon U–Pb Dating

In total, 250 zircons from each sample of the Cretaceous sedimentary rocks were mounted on adhesive tape, then enclosed in epoxy resin, and polished to around half their original thickness. Cathodoluminescence (CL) images were acquired for zircons with ideal crystal shapes (Figure 3) using a JXA-8100 electron microprobe equipped with a CL3 + CL detector. These images were then used to select high-quality zircons for U–Pb dating.

High-resolution U–Th–Pb and rare earth element zircon analyses were undertaken using laser ablation inductively coupled plasma mass spectrometry (LA-ICP-MS) at the Geological Laboratory of Hefei University of Technology, Hefei, China. The analyses were conducted using an Agilent 7500a ICP-MS (Agilent Technologies, Santa Clara, CA, USA) equipped with a 193 nm Geo-Las2005 laser. A 91500 zircon was used as a reference standard with a NIST SRM 610 silicate glass standard used for calibration. The methodology employed was the same as that described by Yan et al. [47], with uncertainties on individual analyses quoted at the 1σ level. Common Pb corrections employed the approach outlined by Andersen [48]. The U–Pb ages reported in this study are $^{207}Pb/^{206}Pb$ ages for zircons older than 1.0 Ga and $^{206}Pb/^{238}U$ ages for zircons younger than 1.0 Ga. The resulting data are given in the Supplementary Materials, Table S1, and were calculated using the ICP-MS-Data Cal 8.0 [49] and Isoplot 3.14 [50] software packages.

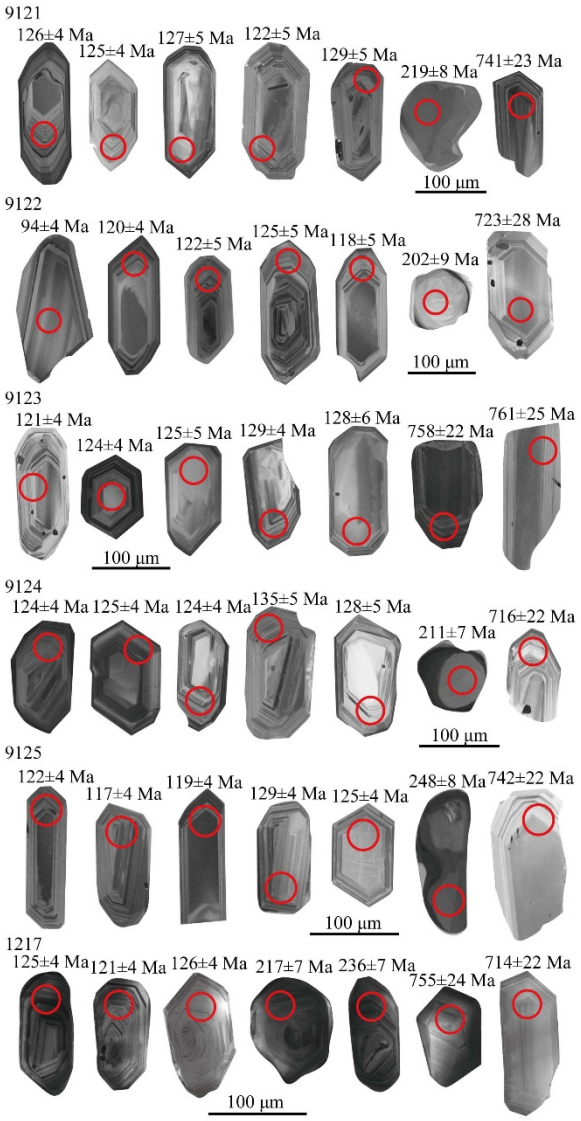

Figure 3. Cathodoluminescence images of selected zircons from sedimentary rocks to the west and east of the ZTB. The red circles indicate analytical sites.

Zircons from the Cretaceous sandstone vary in size from 100 μm to 250 μm (Figure 3). They have abraded and rounded shapes that are indicative of erosion and transportation as detrital zircons. Most zircons show clear oscillatory zoning in CL images and have Th/U ratios significantly greater than 0.1 (Supplementary Materials Table S1), except for some Triassic zircons; thus, they are interpreted to be magmatic in origin [51]. A few of these zircons have complex multiple core–mantle–rim textures with small relict cores visible during imaging, and >95 zircons from each sample yielded age data with 90–100% concordance (Figure 4).

The zircons from six samples gave similar ages that exhibit an Early Cretaceous major cluster, with a few from the Neoproterozoic age. The early Cretaceous clusters were 127 Ma (samples 9121, 9123, and 9124), 121 Ma (sample 9122), 124 Ma (sample 9125), and 125 Ma (sample 1217), respectively; the Neoproterozoic clusters were between 754 Ma and 713 Ma (Figure 4). Some differences are that some middle Paleoproterozoic ages were in sample 9124, while a few earlier Late Cretaceous ages were in sample 9122 with a cluster age of 92 Ma, and there were more Triassic ages in sample 1217 with cluster ages of 217 and 249 Ma (Figure 4).

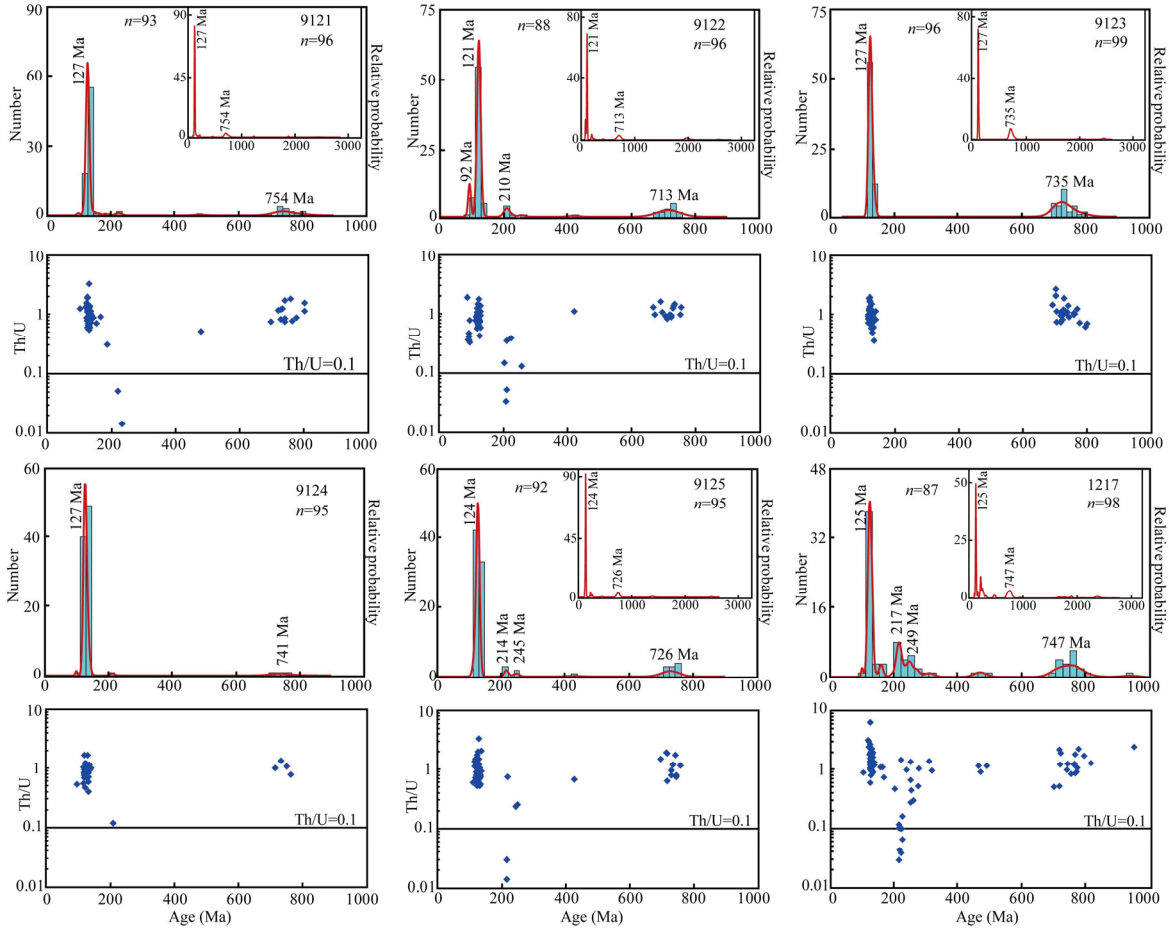

Figure 4. Histograms and relative probability curves of concordant detrital zircon ages on the upper (showing whole age spectra in the boxes) and plots of Th/U ratios versus ages on the bottom for sandstone samples of the Cretaceous sediments adjacent to the ZTB.

4.2. Zircon (U–Th)/He Geochronology and Thermal History Modeling

ZHe dating was undertaken at the $^{40}Ar/^{39}Ar$ and (U–Th)/He geochronology laboratory of the Institution of Geology and Geophysics, Chinese Academy of Sciences (IGGCAS), Beijing, China. A fully automatic He extraction system, Alphachron Mk II (Australian Scientific Instruments Pty Limited), was used to measure the He contents of zircon grains. The system consists of a 970 nm diode laser and a Quadrupole PrismaPlus QMG 220 (Pfeiffer Vacuum). For this, 3–5 euhedral zircon grains, free of visible inclusions or internal cracks (Figure 5), were selected from each sample and measured under a microscope. The methodology employed was the same as that described by Wu et al. [52], with uncertainties on individual analyses quoted at the 1σ level. The resulting data are given in Table 1.

A low helium content of one grain in sample 1603 resulted in an abnormal age result, while the other two grains obtained ages of 95.9 ± 5.1 Ma and 83.4 ± 4.4 Ma, with a weighted mean age of 89.0 ± 4.8 Ma (Table 1). Samples 1605 and 1618 all obtained age results for four grains, with weighted mean ages of 112.0 ± 6.1 Ma and 79.2 ± 4.2 Ma, respectively. Samples 1608, 1614, and 1619 obtained age results for three grains, with weighted mean ages of 102.0 ± 5.5 Ma, 125.1 ± 6.6 Ma, and 103.7 ± 6.2 Ma, respectively (Table 1). In this study, a sample was also collected from the Machang pluton for ZHe dating, but the results of the three grains were abnormal due to either a low helium content or a low thorium and uranium content; thus, these data are not listed in Table 1.

Table 1. Zircon (U–Th)/He ages of the Early Cretaceous intrusion rocks in the ZTB.

Sample	^{238}U (mol)	Std. ^{238}U (mol)	^{232}Th (mol)	Std. ^{232}Th (mol)	^{4}He (mol)	Std. ^{4}He (mol)	Age_{Raw} Ma ± 1σ	Ft	Age_{Cor} Ma ± σ	Th/U
1603-1	6.9539×10^{-12}	1.0991×10^{-13}	6.7816×10^{-12}	7.6333×10^{-14}	8.0938×10^{-13}	9.8184×10^{-15}	73.6 ± 1.3	0.77	95.9 ± 5.1	1.0
1603-2	6.1666×10^{-12}	9.8630×10^{-14}	5.6123×10^{-12}	6.0194×10^{-14}	6.3447×10^{-13}	7.8330×10^{-15}	65.9 ± 1.2	0.79	83.4 ± 4.4	0.9
1603-3	5.4560×10^{-12}	8.9991×10^{-14}	5.2173×10^{-12}	4.9895×10^{-14}	7.4149×10^{-15}	9.2885×10^{-17}	0.87 ± 0.02	0.76	1.15 ± 0.06	0.9
	Weighted mean age								89.0 ± 4.8	
1605-1	5.0698×10^{-12}	8.0805×10^{-14}	3.4876×10^{-12}	3.3286×10^{-14}	5.8970×10^{-13}	7.2903×10^{-15}	77.8 ± 1.4	0.73	106.0 ± 5.6	0.7
1605-2	7.9180×10^{-12}	1.2306×10^{-13}	5.0780×10^{-12}	4.1724×10^{-14}	9.7828×10^{-13}	1.1686×10^{-14}	83.3 ± 1.5	0.74	112.2 ± 6.0	0.6
1605-3	4.3936×10^{-12}	6.9728×10^{-14}	4.2304×10^{-12}	3.7144×10^{-14}	5.3905×10^{-13}	6.5139×10^{-15}	77.8 ± 1.4	0.72	107.7 ± 5.7	1.0
1605-4	6.1658×10^{-12}	1.6126×10^{-13}	3.7717×10^{-12}	1.1905×10^{-13}	8.4511×10^{-13}	1.0156×10^{-14}	92.9 ± 2.4	0.72	128.4 ± 7.2	0.6
	Weighted mean age								112.0 ± 6.1	
1608-1	4.5010×10^{-12}	7.5045×10^{-14}	4.1332×10^{-12}	7.8473×10^{-14}	5.2204×10^{-13}	6.1575×10^{-15}	74.2 ± 1.4	0.74	100.5 ± 5.4	0.9
1608-2	5.9795×10^{-12}	9.5895×10^{-14}	4.8547×10^{-12}	4.5224×10^{-14}	6.6290×10^{-13}	7.2182×10^{-15}	72.4 ± 1.3	0.77	93.9 ± 5.0	0.8
1608-3	2.2334×10^{-12}	3.6706×10^{-14}	1.6076×10^{-12}	1.4088×10^{-14}	2.9619×10^{-13}	3.5428×10^{-15}	88.0 ± 1.6	0.75	117.1 ± 6.2	0.7
	Weighted mean age								102.0 ± 5.5	
1614-1	2.3177×10^{-12}	3.8637×10^{-14}	1.1829×10^{-12}	1.5988×10^{-14}	2.8215×10^{-13}	3.4498×10^{-15}	84.3 ± 1.6	0.69	123.1 ± 6.6	0.5
1614-2	2.7446×10^{-12}	4.8454×10^{-14}	1.2574×10^{-12}	1.3731×10^{-14}	3.2534×10^{-13}	3.6368×10^{-15}	83.0 ± 1.6	0.69	120.5 ± 6.5	0.5
1614-3	7.6191×10^{-12}	1.1884×10^{-13}	2.7176×10^{-12}	2.4884×10^{-14}	1.0598×10^{-12}	1.2008×10^{-14}	99.4 ± 1.8	0.77	129.4 ± 6.9	0.4
1614-4	4.0019×10^{-12}	6.4119×10^{-14}	1.6834×10^{-12}	1.9378×10^{-14}	5.0632×10^{-13}	6.1193×10^{-15}	89.3 ± 1.7	0.70	128.1 ± 6.8	0.4
	Weighted mean age								125.1 ± 6.6	
1618-1	2.4202×10^{-12}	4.0810×10^{-14}	2.4009×10^{-12}	3.0478×10^{-14}	2.4002×10^{-13}	2.9021×10^{-15}	62.6 ± 1.2	0.80	78.0 ± 4.2	1.0
1618-2	2.1072×10^{-12}	3.4269×10^{-14}	2.3479×10^{-12}	2.4494×10^{-14}	2.1578×10^{-13}	2.3532×10^{-15}	63.2 ± 1.1	0.81	78.1 ± 4.1	1.1
1618-3	2.9706×10^{-12}	5.0201×10^{-14}	3.2157×10^{-12}	2.8955×10^{-14}	3.1955×10^{-13}	3.9428×10^{-15}	66.8 ± 1.2	0.83	80.8 ± 4.3	1.1
1618-4	1.7310×10^{-12}	2.7304×10^{-14}	1.8712×10^{-12}	1.8843×10^{-14}	1.7529×10^{-13}	2.1261×10^{-15}	62.9 ± 1.1	0.78	80.3 ± 4.3	1.1
	Weighted mean age								79.2 ± 4.2	
1619-1	8.3687×10^{-12}	1.3367×10^{-13}	5.6124×10^{-12}	4.9783×10^{-14}	1.0769×10^{-12}	1.3182×10^{-14}	86.3 ± 1.6	0.79	108.9 ± 5.8	0.7
1619-2	3.3856×10^{-12}	5.5237×10^{-14}	2.7304×10^{-12}	3.0972×10^{-14}	4.0209×10^{-13}	4.2709×10^{-15}	77.6 ± 1.4	0.75	103.2 ± 5.5	0.8
1619-3	3.6062×10^{-12}	5.8500×10^{-14}	1.9031×10^{-12}	3.2775×10^{-14}	3.7676×10^{-13}	4.2359×10^{-15}	72.2 ± 1.3	0.72	99.8 ± 5.3	0.5
	Weighted mean age								103.7 ± 6.2	

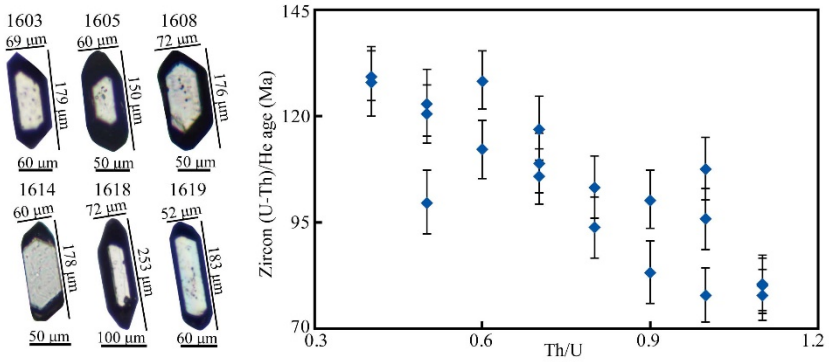

Figure 5. Left: Photomicrographs of selected zircon grains showing their lengths and widths. **Right**: Single-crystal zircon (U–Th)/He age versus Th/U ratio.

HeFTy version 1.90 [53] and a MonteCarlo method were used to invert for the low-temperature thermal history of the ZTB. The weighted mean age from each sample was used. In the thermal history modeling, 20 °C was set as the initial surface temperature, and 180 °C, the closure temperature of zircon He systems [54], was set as the temperature constraint. The models started with the emplacement of the intrusion rocks (~129 Ma) and terminated when 300 good paths (goodness of fit >0.5) were found. The thermal history inversion results are shown as path envelopes in Figure 6. All acceptable paths (goodness of fit >0.05) constitute the green area, all good paths constitute the magenta area, and the solid black line represents the best-fit path.

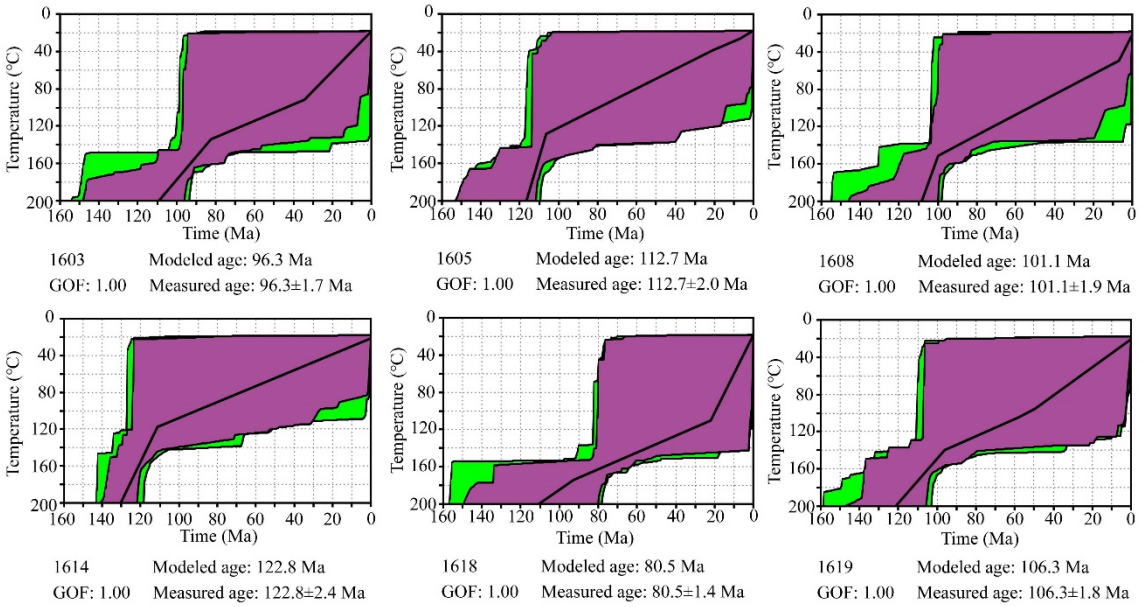

Figure 6. Thermal histories of magmatic samples from the ZTB modeled using HeFTy version 1.90. Here, 0 Ma and 20 °C are the present time and presumed surface temperature, respectively. The green and magenta areas contain all the acceptable and good evolutionary paths, respectively. The black line shows the best-fit evolutionary path. The measured age, the age modeled using HeFTy, and the goodness of fit (GOF) are displayed in each figure. The GOF was used to assess the fit between the modeled and measured ages, with values of >0.50 indicating a good fit.

The simulation results (Figure 6) show that samples 1603 and 1608 yielded rapid cooling, followed by slow cooling, and finally rapid cooling. The difference is that sample 1603 showed relatively rapid cooling of 2.3 °C/Ma after 30 Ma, while sample 1608 exhibited rapid cooling after 10 Ma with cooling rate of 4 °C/Ma. Samples 1605, 1614, and 1619 exhibited similar patterns, where rapid cooling was followed slow cooling. Sample 1618

cooled rapidly at 100 Ma, followed by slow cooling, and then rapid cooling of 5 °C/Ma after 20 Ma.

5. Discussion

5.1. Provenance Analysis of the Upper Cretaceous

The ZTB mainly crops out the Zhangbaling Group and the Feidong Complex, of which protoliths of the Feidong Complex and metavolcanic rocks of the Zhangbaling Group are mainly middle Neoproterozoic magmatic rocks [26,28,39] and a few Paleoproterozoic rocks [27,29]. The metasediments of the Zhangbaling Group are also mainly derived from the middle Neoproterozoic magmatic rocks [26]. Therefore, the ZTB exhibits a distinctive age–frequency distribution with a major cluster of the middle Neoproterozoic (Figure 7). The eruption time of Early Cretaceous volcanic rocks in the Chuzhou area to the east of the ZTB range from 132 to 116 Ma [40,41], mainly around 125 Ma (Figure 7). The ages of intrusion rocks along the Tan–Lu Fault Zone range from 132 Ma to 122 Ma, and most of them range from 130 Ma to 128 Ma (Figure 1). The compilation of these ages provides the basis for provenance analysis of the Cretaceous strata to the west and east of the ZTB.

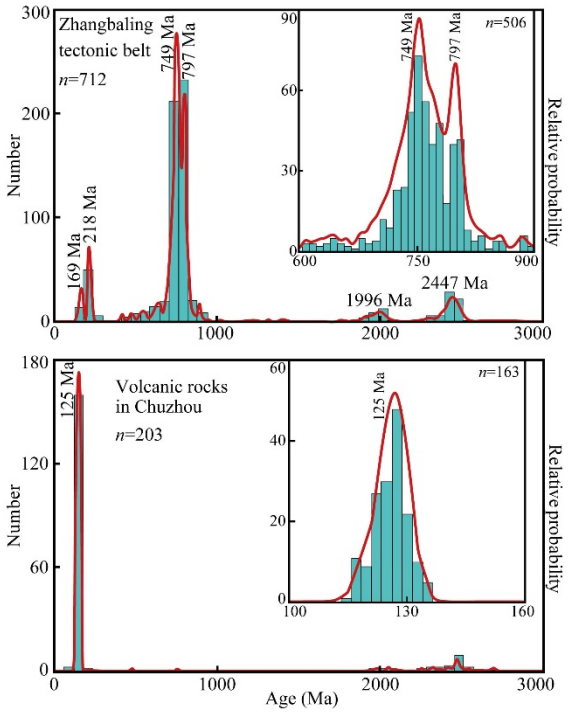

Figure 7. Compilations of concordant zircon U–Pb ages for the ZTB and the Chuzhou volcanic rocks. Data for the ZTB are from Zhao et al. [26], Shi [27], Cai et al. [28], and Yuan et al. [29]; data for the Chuzhou volcanic rocks are from Xie et al. [40] and Ma and Xue [41].

The Upper Cretaceous Zhangqiao Formation is mainly distributed along the nearly E–W Feizhong Fault and Lu'an Fault, and partly exposed in the northeastern Hefei Basin, which were controlled by the normal fault activities of the Shouxian–Dingyuan Fault and Tan–Lu Fault Zone [46]. Previous studies showed that the source materials of the Zhangqiao Formation adjacent to the ZTB came from rocks within this belt [25,44]. Therefore, if the source materials of samples came from the Zhangbaling Group and the Feidong Complex, the age–frequency distributions of the sediments should show a distinctive major cluster of the middle Neoproterozoic. However, our new detrital zircon age–frequency data showed a single Early Cretaceous major cluster with a few middle Neoproterozoic ages (Figure 4), although the Upper Cretaceous conglomerate contains clasts of gneiss and phyllite. Moreover, the Upper Cretaceous showed similar age–frequency distributions to those of the Lower Cretaceous, indicating that the rocks exposed in the ZTB during

the whole Cretaceous did not change, thus providing the same source materials for the sediments on the two sides.

Detailed field work showed that the Lower Cretaceous strata at the margin of the basin were not directly covered on the Zhangbaling Group; rather, Early Cretaceous volcanic rocks covered the Zhangbaling Group or the Paleozoic strata, and volcanic rocks were then covered by the Cretaceous strata. Obviously, in the earlier Late Cretaceous, the Early Cretaceous volcanic rocks covered the Feidong Complex and the Zhangbaling Group and provided source materials for the Upper Cretaceous, which caused a single Early Cretaceous cluster in sediments on both sides of the ZTB. In this work, the location of the collected sediments to the west of ZTB covered the whole northern Zhangbaling (Figure 1); hence, the similar age–frequency distributions of all samples indicate that the whole ZTB was covered by volcanic rocks in the earlier Late Cretaceous. The Early Cretaceous plutons on the western margin of the ZTB are one potential provenance for the Upper Cretaceous strata [25], but the thermal history inversion results showed that these plutons may have cooled to around 100 °C in the earlier Late Cretaceous and may not have been exposed on the surface. Moreover, these plutons intruded into the Feidong Complex and the Zhangbaling Group and were unable to provide single Early Cretaceous source materials for sediments. On the basis of the above analysis, it can be concluded that source materials of the Upper Cretaceous strata came mainly from the Early Cretaceous volcanic rocks.

5.2. Tectonic Uplift of the Zhangbaling Tectonic Belt

The $^{40}Ar/^{39}Ar$ age of the Wawuliu, Wawuxue, and Guandian plutons in the northern Zhangbaling were between 127.8 Ma and 122.9 Ma, respectively [36], which are close to their zircon U–Pb ages (Figure 1), indicating that these plutons were emplaced at relatively shallow depths. Throughout the whole Lower Yangtze Region, the emplacement depth of ore-forming plutons was all obviously shallow [55], and their wall rocks were mainly the Paleozoic strata, which typically caused the $^{40}Ar/^{39}Ar$ results to be similar to their zircon U–Pb ages [56]. Sample 1614 collected from the Huangdaoshan pluton to the east of the ZTB yielded a (U–Th)/He age of 122.8 Ma, slightly younger than its zircon U–Pb age (Figure 6). This pluton was located in the Lower Yangtze Region and may also have a relatively shallow emplacement depth, resulting in its zircon (U–Th)/He age being close to its zircon U–Pb age.

The Lower Cretaceous Zhuxiang Formation and Upper Cretaceous Zhangqiao Formation are widely developed in the eastern Hefei Basin, while the Lower Cretaceous Xiangdaopu Formation, developing between these two strata, is only developed in the northeast corner of the Hefei Basin [46]. During sedimentation of the Xiangdaopu Formation, certain uplift occurred in the northern Zhangbaling as the footwall of the normal Tan–Lu Fault. The wall rocks of the Wawuxue pluton are the lower part of the Zhangbaling Group, while those of the Wawuliu and Guandian plutons are the upper part [26,32], indicating that the Wawuxue pluton (sample 1605) has a larger uplift, thus recording an earlier cooling time (112.7 Ma). Correspondingly, the Qiaotouji pluton (sample 1618), intruding into the orthogneiss of the Feidong Complex, obtained the minimum cooling age (80.5 Ma). It was the unique diorite in all selected samples, and its smaller cooling age may be related to the larger emplacement depth.

Samples 1608, 1603, and 1619, rapidly cooling at around 100 Ma, were distributed in the northern, middle, and southern part of the ZTB (Figure 5), indicating that a rapid cooling event occurred around 100 Ma throughout the ZTB. Usually, conglomerate sedimentation is related to the uplifting of adjacent tectonic belt [57]. The lower part of the Upper Cretaceous Zhangqiao Formation is an alluvial fan deposit [44] and distributed along the west flank of the ZTB, which indicates that the ZTB experienced rapid uplift in the earlier Late Cretaceous.

Detailed field observation showed that the southern Zhangbaling mainly recorded three stages of late Mesozoic tectonic activities, namely, sinistral strike–slip, thrust, and normal activity. The sinistral strike–slip shear zone developed mainly in the orthogneiss

of the Feidong Complex, while the marble of the Feidong Complex usually shows brittle thrusting and is not superimposed by the sinistral strike–slip fault. Because marbles are mainly distributed to the south of the orthogneiss along the strike, it can be inferred that development of the thrust fault should be after the sinistral strike–slip fault, and the marbles exposed on the surface were more likely to be rocks overthrusted from the hanging wall. Many of the $^{40}Ar/^{39}Ar$ ages of mylonite and the zircon U–Pb ages of undeformed dikes indicate that the sinistral strike–slip shear zone in the Feidong Complex was formed in the Early Cretaceous [42,46], which limits these thrust faults to being formed since the Early Cretaceous. A thrust fault is also developed in the Machang pluton and Chuzhou volcanic rocks (Figure 2), indicating that the thrusting in the Feidong Complex was not earlier than about 128 Ma. In the ZTB, the normal fault was superimposed on the thrust fault or the strike–slip fault, indicating that the normal fault activity was the latest activity. Given that the Upper Cretaceous strata developed in the eastern Hefei Basin is a consequence of the normal activity of the Tan–Lu Fault Zone, these normal faults should correspond to the development of the Hefei Basin in the Late Cretaceous, and the earlier thrust fault may occur in the mid-Cretaceous.

It is worth noting that samples 1603, 1608, and 1618 all experienced rapid cooling after 30 Ma (Figure 6), which corresponds to the Cenozoic uplifting in East China [8,9,58]. It is held that this uplifting resulted from the E–W compressive stress field by the continent–continent collision between the Indian Plate and the Eurasian Plate. The ZTB should be exposed on the surface, and it formed a watershed after 30 Ma. Therefore, it is believed that the ZTB should be characterized by tectonic uplift resulting from compression and uplift from the 300 °C isothermal plane (closure temperature of biotite K–Ar system) to the 180 °C isothermal plane depth (zircon (U–Th)/He closure temperature), and the present watershed landform was formed after 30 Ma.

5.3. Indications for Mid-Cretaceous Tectonic Evolution in East Asia

Since the Mesozoic, East Asia has been sandwiched by the Siberian Plate, the Indian Plate, and the Paleo-Pacific Plate and has experienced a complex evolution history [2,3]. Many studies have shown that the tectonic evolution of East Asia was mainly controlled by the subduction of the Paleo-Pacific Plate during the late Mesozoic, and large-scale magmatism followed by explosive mineralization occurred in East China [2,13–15,59].

During the mid-Cretaceous, the movement direction of the Pacific Plate rotated about 75° clockwise, changed from SWW to NW, and kept this direction until now [19,21]. Regional angular unconformity between the Upper and Lower Cretaceous widely occurred in the Korean peninsula [16], NE China [18], North China [17], and South China [12]. The regional magmatism in all of East China was significantly weakened. Although the end of the Early Cretaceous magmatism time period is still controversial, this magmatism formed by the subduction of the Pacific Plate extends southward to Borneo, SE Asia, and shows a huge magmatic belt in the eastern part of the Eurasia continent [13,60,61], for which ~100 Ma represents an obvious magmatic quiescence [60]. Our new data also show that the ZTB was dominated by thrust activity in the mid-Cretaceous. Therefore, East Asia should show regional compression in the mid-Cretaceous, and its dynamic mechanism may be related to the low-angle subduction of the Philippines Plate [15] and the Izanagi Plate [46] beneath the Eurasian Plate.

Recently, extensive low-temperature thermochronology work has been carried out in East China. The zircon fission track ages are mainly between 120 and 85 Ma [9,58], and the zircon (U–Th)/He ages are mainly between 100 and 75 Ma [52,62,63]. Although these ages are closely related to the crustal extensional event which formed basin-and-range style topography, the landscape pattern was already very similar to the present. In conclusion, development of the present landscape pattern in East Asia began in the mid-Cretaceous.

6. Conclusions

1. The ZTB was still covered by Early Cretaceous volcanic rocks in the earlier Late Cretaceous and did not show a watershed landscape in East China. In the mid-Cretaceous, the ZTB was characterized by compression uplift dominated by thrust activity and experienced significant uplift. Rapid uplifting after 30 Ma led to the formation of the current watershed landscape.
2. On the basis of the comprehensive analysis of the existing achievements and our new data, it can be inferred that the formation of the current landscape pattern in East Asia should have begun in the mid-Cretaceous, and it may be related to the low-angle westward subduction of the Philippines Plate and the northward subduction of the Izanagi Plate.

Supplementary Materials: The following supporting information can be downloaded at https://www.mdpi.com/article/10.3390/min13091142/s1: Table S1. Detrital zircon LA-ICP-MS U–Pb ages for the Cretaceous sandstones in the ZTB.

Author Contributions: Conceptualization, Q.B. and Y.W.; methodology, W.M.; software, Q.B. and W.M.; validation, Q.B., W.M. and Y.W.; formal analysis, Y.W.; investigation, Y.W., Q.B., W.M. and J.Y.; data curation, Y.W., Q.B. and J.Y.; writing—original draft preparation, Y.W.; writing—review and editing, Y.W. and Z.L.; supervision, Z.L.; project administration, Y.W.; funding acquisition, Y.W. All authors have read and agreed to the published version of the manuscript.

Funding: This research was funded by the National Natural Science Foundation of China (grant numbers 42272240).

Institutional Review Board Statement: Not applicable.

Informed Consent Statement: Not applicable.

Data Availability Statement: The authors confirm that the data supporting the findings of this study are available within the article and its Supplementary Materials.

Acknowledgments: The authors thank Wu Lin (Institution of Geology and Geophysics, Chinese Academy of Sciences) for (U–Th)/He analyses and Wang Fangyue (Geological Laboratory, Hefei University of Technology) for LA-ICP-MS U–Pb dating.

Conflicts of Interest: The authors declare no conflict of interest.

References

1. Yin, A. Cenozoic tectonic evolution of Asia: A preliminary synthesis. *Tectonophysics* **2010**, *488*, 293–325. [CrossRef]
2. Dong, S.W.; Zhang, Y.Q.; Zhang, F.Q.; Cui, J.J.; Chen, X.H.; Zhang, S.H.; Miao, L.C.; Li, J.H.; Shi, W.; Li, Z.H.; et al. Late Jurassic–Early Cretaceous continental convergence and intracontinental orogenesis in East Asia: A synthesis of the Yanshan Revolution. *J. Asian Earth Sci.* **2015**, *114*, 750–770.
3. Zhang, Y.Q.; Qiu, E.K.; Dong, S.W.; Li, J.H.; Shi, W. Late Mesozoic intracontinental deformation and magmatism in North and NE China in response to multi-plate convergence in NE Asia: An overview and new view. *Tectonophysics* **2022**, *835*, 229377.
4. Wu, L.; Wang, F.; Yang, J.H.; Wang, Y.Z.; Zhang, W.B.; Yang, L.K.; Shi, W.B. Meso-Cenozoic uplift of the Taihang Mountains, North China: Evidence from zircon and apatite thermochronology. *Geol. Mag.* **2019**, *157*, 1097–1111. [CrossRef]
5. Hao, Y.Q.; Yu, J.X.; Wang, Y.Z.; Li, C.P.; Pang, J.Z.; Wang, Y.; Zheng, D.W. Coupling between Cenozoic extensional exhumation in North China and the subduction of the Pacific Plate. *Palaeogeogr. Palaeocl.* **2023**, *620*, 111546. [CrossRef]
6. Yang, F.; Santosh, M.; Glorie, S.; Jepson, G.; Xue, F.; Kim, S.W. Meso-Cenozoic multiple exhumation in the Shandong Peninsula, eastern North China Craton: Implications for lithospheric destruction. *Lithos* **2020**, *370–371*, 105597.
7. Hu, S.B.; Kohn, B.P.; Raza, A.; Wang, J.Y.; Gleadow, A.J.W. Cretaceous and Cenozoic cooling history across the ultrahigh pressure Tongbai-Dabie belt, central China, from apatite fission-track thermochronology. *Tectonophysics* **2005**, *420*, 409–429. [CrossRef]
8. Yuan, W.M.; Yang, Z.Q.; Zhang, Z.C.; Deng, J. The uplifting and denudation of main Huangshan Mountains, Anhui Province. *China. Sci. China Earth Sci.* **2011**, *54*, 1168–1176. [CrossRef]
9. Wang, Y.; Wang, Y.J.; Li, S.B.; Seagren, E.; Zhang, Y.Z.; Zhang, P.Z.; Qian, X. Exhumation and landscape evolution in eastern South China since the Cretaceous: New insights from fission-track thermochronology. *J. Asian Earth Sci.* **2020**, *191*, 104239. [CrossRef]
10. van Hinsbergen, D.J.J.; Lippert, P.C.; Dupont-Nivet, G.; McQuarrie, N.; Doubrovine, P.V.; Spakman, W.; Torsvik, T.H. Greater India Basin hypothesis and a two-stage Cenozoic collision between India and Asia. *Proc. Natl. Acad. Sci. USA* **2012**, *109*, 7659–7664. [CrossRef]

11. Ding, L.; Kapp, P.; Cai, F.L.; Garzione, C.N.; Xiong, Z.Y.; Wang, H.Q.; Wang, C. Timing and mechanisms of Tibetan Plateau uplift. *Nat. Rev. Earth Environ.* **2022**, *3*, 652–667. [CrossRef]
12. Li, J.H.; Zhang, Y.Q.; Dong, S.W.; Johnston, S.T. Cretaceous tectonic evolution of South China: A preliminary synthesis. *Earth-Sci. Rev.* **2014**, *134*, 98–136.
13. Yang, Y.Z.; Chen, F.K.; Siebel, W.; Zhang, H.; Long, Q.; He, J.F.; Hou, Z.H.; Zhu, X.Y. Age and composition of Cu-Au related rocks from the lower Yangtze River belt: Constraints on paleo-Pacific slab roll-back beneath eastern China. *Lithos* **2014**, *202–203*, 331–346. [CrossRef]
14. Zhu, R.X.; Zhang, H.F.; Zhu, G.; Meng, Q.R.; Fan, H.R.; Yang, J.H.; Wu, F.Y.; Zhang, Z.Y.; Zheng, T.Y. Craton destruction and related resources. *Int. J. Earth Sci.* **2017**, *106*, 2233–2257. [CrossRef]
15. Wei, W.; Lin, W.; Chen, Y.; Faure, M.; Ji, W.B.; Hou, Q.L.; Yan, Q.R.; Wang, Q.C. Tectonic controls on magmatic tempo in an active continental margin: Insights from the Early Cretaceous syn-tectonic magmatism in the Changle-Nan'ao Belt, South China. *J. Geophys. Res.-Sol. Ea.* **2023**, *128*, e2022JB025973. [CrossRef]
16. Choi, T.; Lee, Y.I. Thermal histories of Cretaceous basins in Korea: Implications for response of the East Asian continental margin to subduction of the Paleo-Pacific Plate. *Island Arc.* **2011**, *20*, 371–385.
17. Suo, Y.H.; Li, S.Z.; Cao, X.Z.; Wang, X.Y.; Somerville, I.; Wang, G.Z.; Wang, P.C.; Liu, B. Mesozoic-Cenozoic basin inversion and geodynamics in East China: A review. *Earth-Sci. Rev.* **2020**, *210*, 103357.
18. Guo, Z.X.; Yang, Y.T. Late Mesozoic basin evolution in NE China and its surrounding areas, mechanisms of the continental-scale extensional regime in East Asia during the Late Jurassic–Early Cretaceous. *Earth Sci. Rev.* **2023**, *241*, 104418. [CrossRef]
19. Matthews, K.J.; Seton, M.; Müller, R.D. A global-scale plate reorganization event at 105–100 Ma. *Earth Planet. Sci. Lett.* **2012**, *355–356*, 283–298.
20. Müller, R.D.; Seton, M.; Zahirovic, S.; Williams, S.E.; Matthews, K.J.; Wright, N.M.; Shephard, G.E.; Maloney, K.T.; Barnett-Moore, N.; Hosseinpour, M.; et al. Ocean basin evolution and global-scale plate reorganization events since Pangea breakup. *Annu. Rev. Earth Planet. Sci.* **2016**, *44*, 107–138. [CrossRef]
21. Olierook, H.K.H.; Jourdan, F.; Whittaker, J.M.; Merle, R.E.; Jiang, Q.; Pourteau, A.; Doucet, L.S. Timing and causes of the mid-Cretaceous global plate reorganization event. *Earth Planet. Sci. Lett.* **2020**, *534*, 116071. [CrossRef]
22. Zhang, Q.; Qian, Q.; Wang, E.Q.; Wang, Y.; Zhao, T.P.; Hao, J.; Guo, G.J. An east China plateau in mid-late Yanshanian period: Implication from adakites. *Chin. J. Geol.* **2001**, *36*, 248–255.
23. Li, H.Y.; Xu, Y.G.; Liu, Y.M.; Huang, X.L.; He, B. Detrital zircons reveal no Jurassic plateau in the eastern North China Craton. *Gondwana Res.* **2013**, *24*, 622–634. [CrossRef]
24. Xu, J.W.; Zhu, G.; Tong, W.X.; Cui, K.R.; Liu, Q. Formation and evolution of the Tancheng-Lujiang wrench fault system: A major shear system to the northern of the Pacific Ocean. *Tectonophysics* **1987**, *134*, 273–310.
25. Zhu, G.; Wang, Y.S.; Wang, W.; Zhang, S.; Liu, C.; Gu, C.C.; Li, Y.J. An accreted micro-continent in the north of the Dabie Orogen, East China: Evidence from dating results of detrital zircons. *Tectonophysics* **2017**, *698*, 47–64. [CrossRef]
26. Zhao, T.; Zhu, G.; Lin, S.Z.; Wang, H.Q. Indentation-induced tearing of a subducting continent: Evidence from the Tan–Lu Fault Zone, East China. *Earth-Sci. Rev.* **2016**, *152*, 14–36. [CrossRef]
27. Shi, Y.H. Petrology and zircon U–Pb geochronology of metamorphic massifs around the middle segment of the Tan-Lu fault to define the boundary between the North and South China blocks. *J. Asian Earth Sci.* **2017**, *141*, 140–160. [CrossRef]
28. Cai, Q.R.; Niu, M.L.; Yuan, X.Y.; Wu, Q.; Zhu, G.; Li, X.C.; Sun, Y.; Li, C. Evidence for continental rifting from two episodes of mid-Neoproterozoic silicic magmatism in the northeastern Yangtze Block, China. *Precambrian Res.* **2021**, *363*, 106336. [CrossRef]
29. Yuan, X.Y.; Niu, M.L.; Cai, Q.R.; Zhu, G.; Wu, Q.; Li, X.C.; Sun, Y.; Li, C.; Qian, T. The nature of Paleoproterozoic basement in the northern Yangtze and its geological implication. *Precambrian Res.* **2022**, *378*, 106761.
30. Zhang, Q.; Teyssier, C.; Dunlap, J.; Zhu, G. Oblique collision between North and South China recorded in Zhangbaling and Fucha Shan (Dabie-Sulu transfer zone). *Geol. Soc. Am.* **2007**, *434*, 167–206.
31. Hu, Z.L.; Yang, X.Y.; Duan, L.A.; Sun, W.D. Geochronological and geochemical constraints on genesis of the adakitic rocks in Outang, South Tan–Lu Fault Belt (Northeastern Yangtze Block). *Tectonophysics* **2014**, *626*, 86–104. [CrossRef]
32. Jia, L.Q.; Mo, X.X.; Santosh, M.; Yang, Z.S.; Yang, D.; Dong, G.C.; Wang, L.; Wang, X.C.; Wu, X. Early Cretaceous continental delamination in the Yangtze Block: Evidence from high-Mg adakitic intrusions along the Tanlu fault, central Eastern China. *J. Asian Earth Sci.* **2016**, *127*, 152–169. [CrossRef]
33. Wang, J.; He, J.; Zhao, J.X.; Yang, Y.Z.; Chen, F.K. Multiple-Stage Neoproterozoic Magmatism Recorded in the Zhangbaling Uplift of the Northeastern Yangtze Block: Evidence from Zircon Ages and Geochemistry. *Minerals* **2023**, *13*, 562. [CrossRef]
34. Li, Y.X.; Yan, J.; Song, C.Z.; Li, C.; Yang, Q.L.; Li, Z.S. Petrogenesis of late Mesozoic granitoids from the southern segment of the Tan–Lu Fault, eastern China: Implications for the tectonic affinity of the Zhangbaling Uplift. *Int. Geol. Rev.* **2021**, *63*, 453–475. [CrossRef]
35. Li, S.Z.; Zhao, G.C.; Zhang, G.W.; Liu, X.C.; Dong, S.W.; Wang, Y.J.; Liu, X.; Suo, Y.H.; Dai, L.M.; Jin, C.; et al. Not all folds and thrusts in the Yangtze foreland thrust belt are related to the Dabie Orogen: Insights from Mesozoic deformation south of the Yangtze River. *Geol. J.* **2010**, *45*, 650–663. [CrossRef]

36. Lin, W.; Faure, M.; Wang, Q.C.; Monié, P.; Panis, D. Triassic polyphase deformation in the Feidong-Zhangbaling Massif (eastern China) and its place in the collision between the North China and South China blocks. *J. Asian Earth Sci.* **2005**, *25*, 121–136. [CrossRef]
37. Lu, Y.C.; Zhu, G.; Yin, H.; Su, N.; Wu, X.D.; Zhang, S.; Xie, C.L. Superposition of two orthogonal transpressions: An example from the oblique convergent margin adjoining the Tan–Lu Fault Zone, eastern China. *Tectonophysics* **2022**, *836*, 229415. [CrossRef]
38. Shi, Y.H.; Zhu, G.; Wang, D.X.; Zhao, Q. Analysis of sodic amphiboles in the blueschists' from the Zhangbaling Group across the central part of Anhui Province and its implication for the metamorphic p-T conditions. *Acta Mineral. Sin.* **2007**, *27*, 179–188.
39. Wang, T.; Niu, M.L.; Wu, Q.; Li, X.C.; Cai, Q.R.; Zhu, G. Episodic bimodal magmatism at an active continental margin due to Paleo-Pacific Plate subduction: A case study from the southern segment of the Tan-Lu Fault Zone, eastern China. *Lithos* **2019**, *328–329*, 159–181. [CrossRef]
40. Xie, C.L.; Zhu, G.; Niu, M.L.; Wang, Y.S. LA-ICP MS zircon U–Pb ages of the Mesozoic volcanic rocks from Chuzhou area and their tectonic significances. *Geol. Rev.* **2007**, *53*, 642–655.
41. Ma, F.; Xue, H.M. SHRIMP zircon U–Pb age of late Mesozoic volcanic rocks from the Chuzhou basin, eastern Anhui Province, and its geological significance. *Acta Petrol. Mineral.* **2011**, *30*, 924–934.
42. Zhu, G.; Wang, Y.S.; Liu, G.S.; Niu, M.L.; Xie, C.L.; Li, C.C. $^{40}Ar/^{39}Ar$ dating of strike-slip motion on the Tan-Lu Fault Zone, East China. *J. Struct. Geol.* **2005**, *27*, 1379–1398. [CrossRef]
43. Liu, S.F.; Heller, P.L.; Zhang, G.W. Mesozoic basin development and tectonic evolution of the Dabieshan orogenic belt, central China. *Tectonics* **2003**, *22*, 1038. [CrossRef]
44. Meng, Q.R.; Li, S.Y.; Li, R.W. Mesozoic evolution of the Hefei Basin in eastern China: Sedimentary response to deformations in the adjacent Dabieshan and along the Tanlu fault. *Geol. Soc. Am. Bull.* **2007**, *119*, 897–916. [CrossRef]
45. Wang, Y.S.; Bai, Q.; Tian, Z.Q.; Du, H. Mesozoic unroofing history of the Dabie Orogen, eastern China: Evidence from detrital zircon geochronology of sediments in the Hefei Basin. *J. Geol.* **2021**, *129*, 183–206. [CrossRef]
46. Zhu, G.; Jiang, D.Z.; Zhang, B.L.; Chen, Y. Destruction of the eastern North China Craton in a backarc setting: Evidence from crustal deformation kinematics. *Gondwana Res.* **2012**, *22*, 86–103. [CrossRef]
47. Yan, H.Y.; Wang, F.Y.; Gu, H.O.; Sun, H.; Ge, C. Geochemical and Sr-Nd-Pb-Hf isotopic characteristics of Muchen pluton in southeast China, constrain the petrogenesis of alkaline A-type magma. *Minerals* **2020**, *10*, 80. [CrossRef]
48. Andersen, T. Correction of Common Lead in U–Pb Analyses that Do Not Report ^{204}Pb. *Chem. Geol.* **2002**, *192*, 59–79. [CrossRef]
49. Liu, Y.S.; Hu, Z.C.; Gao, S.; Günther, D.; Xu, J.; Gao, C.G.; Chen, H.H. In situ analysis of major and trace elements of anhydrous minerals by LA-ICP-MS without applying an internal standard. *Chem. Geol.* **2008**, *257*, 34–43. [CrossRef]
50. Ludwig, K.R. *User's Manual for Isoplot 3.14: A Geochronological Toolkit for Microsoft Excel*; Berkeley Geochronology Center: Berkeley, CA, USA, 2004.
51. Belousova, E.; Griffin, W.; O'Reilly, S.Y.; Fisher, N. Igneous zircon: Trace element composition as an indicator of source rock type. *Contrib. Miner. Pet.* **2002**, *143*, 602–622. [CrossRef]
52. Wu, L.; Monié, P.; Wang, F.; Lin, W.; Ji, W.B.; Yang, L.K. Multi-phase cooling of Early Cretaceous granites on the Jiaodong Peninsula, East China: Evidence from $^{40}Ar/^{39}Ar$ and (U–Th)/He thermochronology. *J. Asian Earth Sci.* **2018**, *160*, 334–347. [CrossRef]
53. Ketcham, R.A. Forward and inverse modeling of low-temperature thermochronology data. *Rev. Mineral. Geochem.* **2005**, *58*, 275–314. [CrossRef]
54. Reiners, P.W.; Spell, T.L.; Nicolescu, S.; Zanetti, K.A. Zircon (U–Th)/He thermochronometry: He diffusion and comparisons with $^{40}Ar/^{39}Ar$ dating. *Geochim. Cosmochim. Acta* **2004**, *68*, 1857–1887. [CrossRef]
55. Liu, Z.F.; Shao, Y.J.; Zhou, H.D.; Liu, N.; Huang, K.X.; Liu, Q.Q.; Zhang, J.D.; Wang, C. Major and Trace Element Geochemistry of Pyrite and Pyrrhotite from Stratiform and Lamellar Orebodies: Implications for the Ore Genesis of the Dongguashan Copper (Gold) Deposit, Eastern China. *Minerals* **2018**, *8*, 380. [CrossRef]
56. Yang, F.; Song, C.Z.; Ren, S.L.; Ji, M.H. The Mesozoic Tectonic Transition from Compression to Extension in the South China Block: Insight from Structural Deformation of the Lushan Massif, SE China. *Minerals* **2022**, *12*, 1531. [CrossRef]
57. Whittaker, A.C.; Attal, M.; Allen, P.A. Characterizing the origin, nature and fate of sediment exported from catchments perturbed by active tectonics. *Basin Res.* **2010**, *22*, 809–828.
58. Wang, Y.; Zuo, R.G.; Cao, K.; Xu, X.B.; Zattin, M. Late Mesozoic to Cenozoic exhumation of the SE South China Block: Constraints from zircon and apatite fission-track thermochronology. *Tectonophysics* **2022**, *838*, 229518. [CrossRef]
59. Lin, W.; Wei, W. Late Mesozoic extensional tectonics in the North China Craton and its adjacent regions: A review and synthesis. *Int. Geol. Rev.* **2018**, *62*, 811–839. [CrossRef]
60. Wang, Y.J.; Qian, X.; Asis, J.B.; Cawood, P.A.; Wu, S.; Zhang, Y.Z.; Feng, Q.L.; Lu, X.H. "Where, when and why" for the arc-trench gap from Mesozoic Paleo-Pacific subduction zone: Sabah Triassic-Cretaceous igneous records in East Borneo. *Gondwana Res.* **2023**, *117*, 117–138. [CrossRef]
61. Zhang, F.F.; Wang, Y.J.; Qian, X.; Cawood, P.A.; Gan, C.S.; Dong, Y.P.; Gao, H.S.; Wang, M.X. Paleo-Pacific subduction in Southeast Vietnam: Evidence from Late Cretaceous intrusive rocks in the Dalat zone. *Lithos* **2023**, *454–455*, 107233. [CrossRef]

62. Liu, X.; Fan, H.R.; Evans, N.J.; Yang, K.F.; Danišík, M.; McInnes, B.I.A.; Qin, K.Z.; Yu, X.F. Exhumation history of the Sanshandao Au deposit, Jiaodong: Constraints from structural analysis and (U–Th)/He thermochronology. *Sci. Rep.* **2017**, *7*, 7787. [CrossRef] [PubMed]
63. Wang, Y.S.; Bai, Q.; Tian, Z.Q.; Lu, S.M.; Li, J.S.; Zhou, Y.Z.; Du, H.; Jiang, C. Exhumation history of Late Mesozoic intrusions in the Tongling-Xuancheng area of the Lower Yangtze region, East China: Evidences from Zircon (U–Th)/He and apatite fission track thermochronology. *Ore Geol. Rev.* **2021**, *135*, 104220. [CrossRef]